

Supplementary Information for

Emergence of a Thorium-Organic Framework as a Radiation Attenuator for Selective X-Ray Dosimetry

Zhaofa Zheng,^{a,b,‡} Huangjie Lu,^{a,b,‡} Xiaofeng Guo,^c Zhengyang Zhou,^d Yumin Wang,^e Zi-Jian Li,^{a,b} Guo-Ping Xiao,^{a,b} Yuan Qian,^{a,b} Jian Lin,^{a,b,*} and Jian-Qiang Wang^{a,b,f,*}

^aShanghai Institute of Applied Physics, Chinese Academy of Sciences, 2019 Jia Luo Road, Shanghai 201800, China. Email: wangjianqiang@sinap.ac.cn (J.Q.W.), linjian@sinap.ac.cn (J.L.).

^bUniversity of Chinese Academy of Sciences No. 19(A) Yuquan Road, Shijingshan District, Beijing, 100049, China

^cDepartment of Chemistry and Alexandra Navrotsky Institute for Experimental Thermodynamics, Washington State University, Pullman, WA 99164-4630, USA

^dShanghai Institute of Ceramics, Chinese Academy of Sciences, Shanghai 200050, P. R. China

^eState Key Laboratory of Radiation Medicine and Protection, School for Radiological and Interdisciplinary Sciences (RAD-X) and Collaborative Innovation Centre of Radiological Medicine of Jiangsu Higher Education Institutions, Soochow University, Suzhou 215123, China.

^fDalian National Laboratory for Clean Energy, Dalian 116023, China

Table of Content

S1. Experimental section.	2
S2. Characterizations.	2
S3. Supplementary Figures.	4
Fig. S1 The TGA plots of Th-SINAP-2 and Htpbz@Th-SINAP-2.	4
Fig. S2 Optical micrographs of X-ray irradiated Htpbz@Th-SINAP-2 before and after being stored under ambient conditions for 48 h.	4
Fig. S3 Optical micrographs of Th-SINAP-2 and Htpbz upon continuous X-ray irradiation.	5
Fig. S4 UV-Vis absorbance spectra of Th-SINAP-2 upon continuous X-ray irradiation.	5
Fig. S5 (a) Correlation between $(A_0 - A)/A_0$ and the X-ray radiation dose. Inlet: linear fit in the low dose range. (b) Standard error of the absorption intensity at 338 nm.	6
Fig. S6 The PXRD patterns of Htpbz@Th-SINAP-2 before and after radiation.	7
Fig. S7 FTIR spectra of Htpbz, Htpbz@Th-SINAP-2 before and after radiation.	7
Fig. S8 SEM images and EDS spectra of Th-SINAP-2 and Htpbz@Th-SINAP-2.	8
S3. Supplementary Tables.	9
Table S1 Crystallographic Data for Th-SINAP-2 and Htpbz@Th-SINAP-2.	9
Table S2 Detection limits of other photochromic materials.	10

S1. Experimental section.

Caution! ^{232}Th used in this study is an α emitter with the daughter of radioactive Ra-228. All thorium compounds used and investigated were operated in an authorized laboratory designed for actinide element studies. Standard precautions for handling radioactive materials should be followed.

Reagents. $\text{Th}(\text{NO}_3)_4 \cdot 6\text{H}_2\text{O}$ (99%, Changchun Institute of Applied Chemistry, Chinese Academy of Sciences), 4-([2,2':6',2''-terpyridine]-4'-yl) benzoic acid (Jilin Chinese Academy of Sciences - Yanshen Technology Co., Ltd), formic acid ($\geq 99.5\%$, Fisher), and N, N'-dimethylformamide (DMF, water ≤ 50 ppm, Adamas) were used as received from commercial suppliers without further purification.

Synthesis of Th-SINAP-2 and Htpbz@Th-SINAP-2. For Th-SINAP-2, a mixture of $\text{Th}(\text{NO}_3)_4 \cdot 6\text{H}_2\text{O}$ (0.01 mmol, 0.0059 g), 40 μL HCOOH, 2 mL DMF, and 100 μL deionized water were loaded into 5 mL glass vials. The vials were sealed and heated to 100°C for 24 hours followed by cooling to room temperature under ambient condition. Colourless tablet crystals of Th-SINAP-2 were isolated after being washed with ethanol and allowed to air-dry at room temperature. The yield of Th-SINAP-2 was calculated to be 80% based on Th. For Htpbz@Th-SINAP-2, a mixture of $\text{Th}(\text{NO}_3)_4 \cdot 6\text{H}_2\text{O}$ (0.01 mmol, 0.0059 g), Htpbz (0.01 mmol, 0.0035g), 40 μL HCOOH, 2 mL DMF, and 100 μL deionized water were loaded into 5 mL glass vials. The vials were sealed and heated to 100°C for 7 days, followed by cooling to room temperature under ambient condition. Large tablet crystals of Htpbz@Th-SINAP-2 were isolated after being washed with ethanol and allowed to air-dry at room temperature. The yield of Htpbz@Th-SINAP-2 was calculated to be 83% based on Th.

S2. Characterizations.

X-ray crystallography. Single-crystal X-ray diffraction data were collected on a Bruker D8-Venture single-crystal X-ray diffractometer equipped with a Turbo X-ray Source (Mo $K\alpha$ radiation, $\lambda = 0.71073 \text{ \AA}$) and a CMOS detector at room temperature. The data frames were collected using the program APEX3 and processed using the SAINT routine. The structures were solved by direct methods and refined by the full-matrix least squares on F^2 using the SHELXTL-2014 program. All non-H atoms were refined with anisotropic displacement parameters. Selected crystallographic information is listed in Table S1. Atomic coordinates and additional structural information are provided in the CIFs (Supporting Information). Powder patterns were collected from 5° to 50°, with a step of 0.02° using a Bruker D8 advance X-ray diffractometer with Cu- $K\alpha$ radiation ($\lambda = 1.54056 \text{ \AA}$) equipped with a Lynxeye one-dimensional detector.

UV-Vis and Fluorescence Spectroscopy. UV-Vis data were acquired from single crystals of all compounds using a Craic Technologies microspectrophotometer. Crystals were placed on quartz slides under Krytox oil, and the data were collected from 200 to 800 nm. The exposure time was auto optimized by the Craic software. Fluorescence spectra were obtained using 365 nm light for excitation.

Fourier Transform Infrared (FTIR) Spectroscopy. The IR spectra were recorded on ground samples using a FTIR spectrometer instrument in the range of 400-4000 cm^{-1} (Thermo Nicolet 6700 spectrometer), equipped with a diamond attenuated total reflectance (ATR) accessory.

Thermogravimetric Analysis (TGA). TGA was carried out in an N₂ atmosphere with a heating rate of 10 °C/min from 30 °C to 900 °C on a NETZSCH STA 449 F3 Jupiter instrument.

Electron Spin-Resonance (ESR) spectroscopy. The electron spin-resonance spectroscopy for nonirradiated and irradiated samples was recorded in JEOL-FA200 spectrometer. An X-band spectrometer (JES-FA200) with 100-kHz field modulation was interfaced with a computer to manipulate the spectra and integrate spectral intensity ESR measurements were performed at room temperature and the microwave power used was 1.0 mW.

Scanning Electron Microscopy and Energy-Dispersive X-ray Spectrometry (SEM-EDS) Analysis. SEM images and EDS data were recorded on a Zeiss Merlin Compact LEO 1530 VP scanning electron microscope. The energy of the electron beam voltage was 5 keV for imaging and 20 keV for quantitative identifications of elements. Samples were attached directly onto carbon conductive tape.

S3. Supplementary Figures.

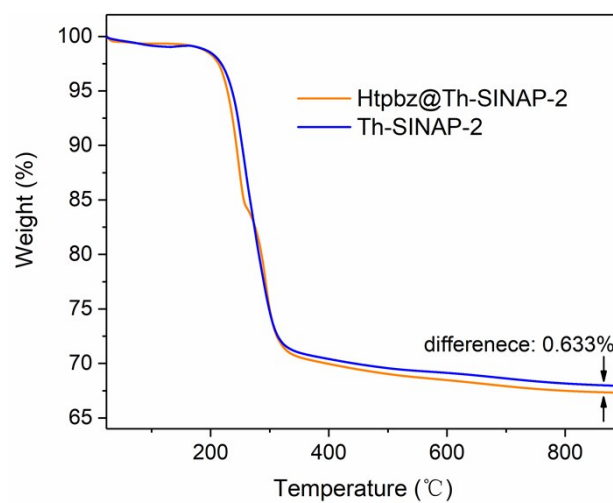


Fig. S1 The TGA plots of Th-SINAP-2 and Htpbz@Th-SINAP-2.

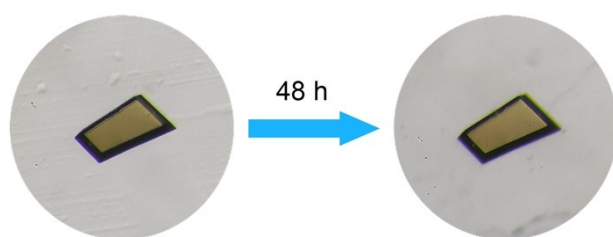


Fig. S2 Optical micrographs of X-ray irradiated Htpbz@Th-SINAP-2 before and after being stored under ambient conditions for 48 h.

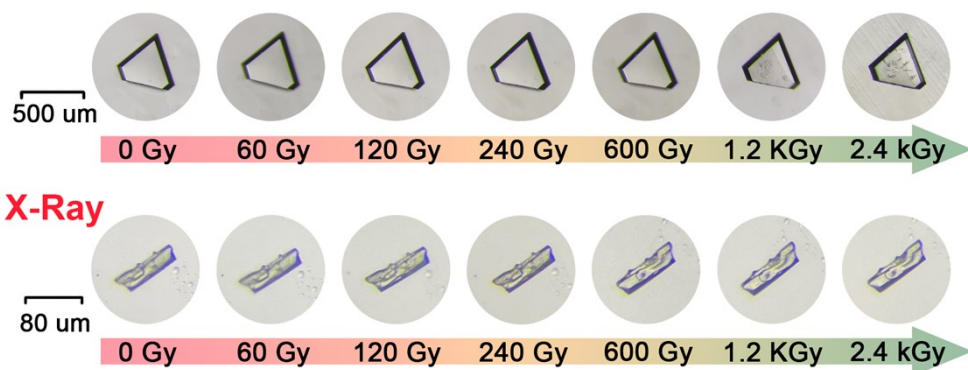


Fig. S3 Optical micrographs of Th-SINAP-2 and Htpbz upon continuous X-ray irradiation.

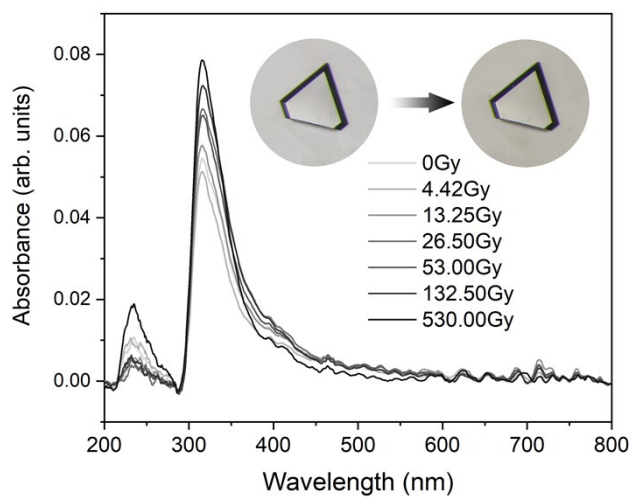


Fig. S4 UV-Vis absorbance spectra of Th-SINAP-2 upon continuous X-ray irradiation..

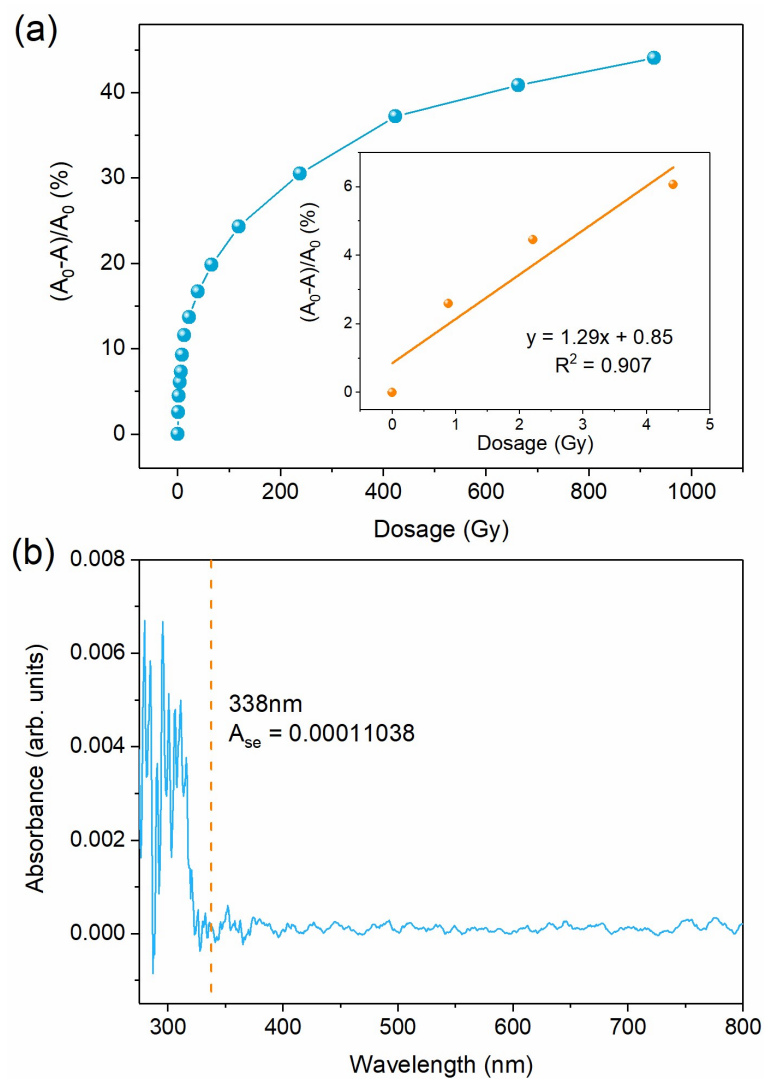


Fig. S5 (a) Correlation between $(A_0 - A)/A_0$ and the X-ray radiation dose. Inlet: linear fit in the low dose range. (b) Standard error of the absorption intensity at 338 nm.

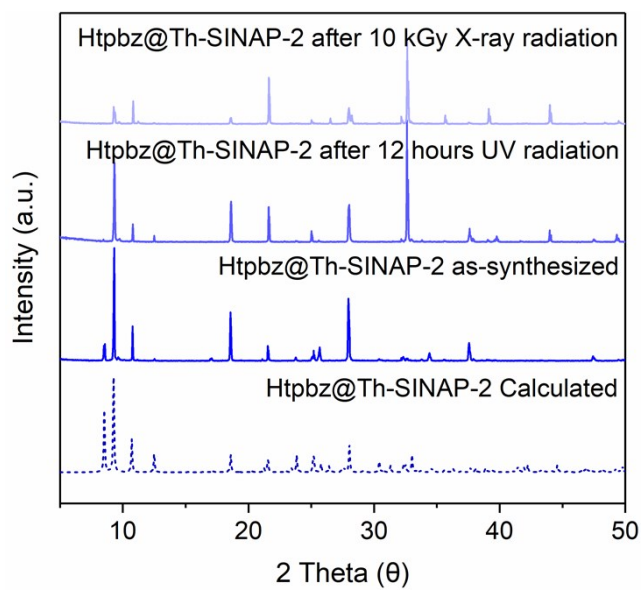


Fig. S6 The PXRD patterns of Htpbz@Th-SINAP-2 before and after radiation.

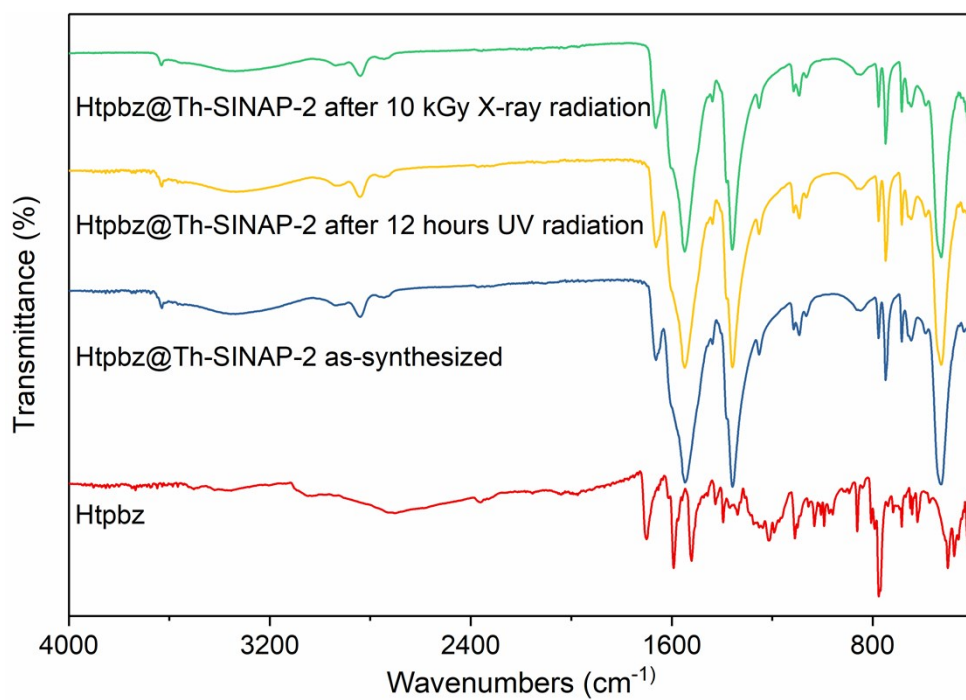


Fig. S7 FTIR spectra of Htpbz, Htpbz@Th-SINAP-2 before and after radiation.

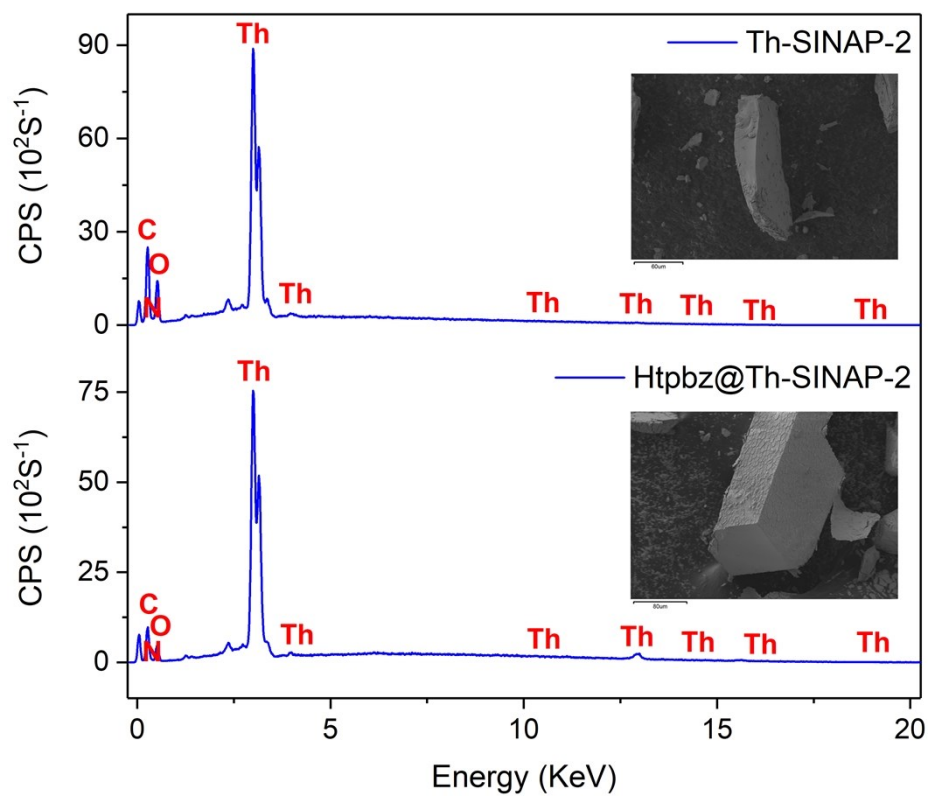


Fig. S8 SEM images and EDS spectra of Th-SINAP-2 and Htpbz@Th-SINAP-2.

S3. Supplementary Tables.

Table S1 Crystallographic Data for Th-SINAP-2 and Htpbz@Th-SINAP-2.

Compound	Th-SINAP-2	Htpbz@Th-SINAP-2
formula	C ₉ H ₄ Th ₃ NO ₁₇	C ₉ H ₄ Th ₃ NO ₁₇
formula weight	1094.25	1094.25
space Group	<i>F m m m</i>	<i>F m m m</i>
a (Å)	16.5124(4)	16.5096(3)
b (Å)	20.7448(6)	20.7464(4)
c (Å)	14.1639(5)	14.1607(3)
α (deg)	90	90
β (deg)	90	90
γ (deg)	90	90
V (Å ³)	4851.8(3)	4850.25(16)
Z	8	8
T (K)	120(2)	120(2)
λ (Å)	0.71073	0.71073
Max. 2 θ (°)	55.02	55.02
ρ_{calcd} Mg/m ³	2.985	2.986
μ (mm ⁻¹)	18.414	18.420
GoF on F ²	1.067	1.170
R_I ,	0.0269,	0.0280,
wR_2 [$I > 2\sigma(I)$]	0.0638	0.0803
R_I ,	0.0308,	0.0300,
wR_2 (all data)	0.0654	0.0817
$(\Delta\rho)_{\text{max}}$,	3.226/	2.977/
$(\Delta\rho)_{\text{min}}/e$ (Å ⁻³)	-2.976	-3.413

Table S2 Detection limits of other photochromic materials.

Material	Detection Limit	References
BaFCl:Eu ²⁺ Polystyrene	1.2 Gy	{Kinashi, 2018 #4794}
[Co(Bpybc) _{1.5} (H ₂ O) ₃]·NO ₃ ·OH·11H ₂ O	7.72 Gy	{Chen, 2017 #4287}
Htpbz@Th-SINAP-2	0.047 Gy	This work